Available online at www.sciencedirect.com
ScienceDirect
Journal of Molecular Catalysis A: Chemical 273 (2007) 224–229
JOURNAL OF MOLECULAR CATALYSIS A: CHEMICAL
www.elsevier.com/locate/molcata

Photocatalytic oxidation of organic dyes by nano-sized metal molybdate incorporated titanium dioxide ($M_xMo_xTi_{1-x}O_6$) (M = Ni, Cu, Zn) photocatalysts

T.K. Ghorai [a,b,c], D. Dhak [b,d], S.K. Biswas [b], S. Dalai [a], P. Pramanik [b,*]

[a] Department of Chemistry and Chemical Technology, Vidyasagar University, Midnapore 721102, India
[b] Department of Chemistry, Indian Institute of Technology, Kharagpur 721302, India
[c] Department of Chemistry, Bajkul Milani Mahavidyalaya, Bajkul, Purba Medinipur 721655, India
[d] Department of Chemistry, Serampore College, Hoogly 712201, India

Received 1 February 2007; received in revised form 29 March 2007; accepted 31 March 2007
Available online 6 April 2007

Abstract

Different metal molybdates incorporated titanium dioxide were prepared by the chemical solution decomposition (CSD) method. Among many transition-metal molybdates, nickel molybdate incorporated titanium dioxide (NMTI) was found to be more photoactive than P25 TiO_2 and other metal molybdate doped TiO_2 ($M_xMo_xTi_{1-x}O_6$) (M = Ni, Cu, Zn; $x = 0.05$), for photocatalytic oxidation of various dyes solution to harmless decolorized solution at room temperature with the help of Hg lamp. The prepared nano powders were characterized by XRD, UV–vis spectra, specific surface area (BET), UV–vis diffuse reflectance spectrum, EPR spectrum and TEM analyses. The average particle size of NMT1 was found to be 15 nm measured from TEM and calculated band gap from adsorption edge is found to be 2.66 eV.

Keywords: Metal molybdate; Titanium dioxide; Nanoparticle; Photochemical reaction

1. Introduction

The photo-catalytic oxidation of organic compounds and dye molecules is an active area of present day's research. In this context, the catalytic oxidation of organic dyes has been investigated extensively [1–4]. Photocatalytic oxidation of various organic dyes (methyl orange, rhodamine B, thymol blue and bromocresol green) may occur even under mild conditions in presence of air and visible light.

During the last 20th years, there are many studies on nano-structured materials due to their several interesting properties like electronic [5] (semiconductor/superconductor), ferroelectric material [6,7], mesoporous material [8], fluorescence [9] and different types of catalytic materials [10,11]. Nano-structured materials have been developed and used as heterogenous catalysts for various applications including the remediation of waste water and air [12] through photocatalytic reaction. Photo catalysis works on photo generation of electrons (e^-) and holes (h^+) when subjected to UV light [13], and their migration of (e^-/h^+ pairs) to the catalyst surface, resulting in the chemical reaction with adsorbed pollutants and oxygen from air. The most extensively studied nano-structured photocatalyst is TiO_2, which has been found to be capable of decomposing many organic contaminants in the liquid phase, gas phase and solid phase. Moreover, TiO_2 photocatalyst as a wide band-gap semiconductor (3.2 eV), is responsive to light radiation in the UV and near UV range ($\lambda < 388$ nm). This limits its application in range of visible light of solar spectrum [14]. To activate TiO_2 in wide visible zone of solar spectrum, doping with various metal ions have been attempted. Many transition metal ions have been used for doping TiO_2 [11–13] to increase the quantum efficiency of the heterogeneous photocatalytic property by influencing generation and recombination of the charge carriers under light. In this regard, CdS-sensitized TiO_2 [15], $(Sr_{1-x}La_x)TiO_{3+\delta}$–$TiO_2$ [16], $BaTi_4O_9$ [17], TiO_2-copper(II) [18], $Na_2Ti_6O_{13}$ [19], Fe(III) doped TiO_2 [20] and La (Fe)-doped bismuth titanate [21] have been extensively investigated.

* Corresponding author. Tel.: +91 3222 283322; fax: +91 3222 255303.
E-mail address: pramanik@chem.iitkgp.ernet.in (P. Pramanik).

1381-1169/$ – see front matter © 2007 Elsevier B.V. All rights reserved.
doi:10.1016/j.molcata.2007.03.075

In this communication, we have attempted the modification of TiO_2 with various metal molybdates ($M_xMo_xTi_{1-x}O_6$) (M = Ni, Cu, Zn; $x = 0.05$) to form nano-sized photocatalyst and their evaluations as photo catalyst. The nano size has helped the formation of solid solution of TiO_2 and metal molybdates and retains high surface area. The $Ni_xMo_xTi_{1-x}O_6$ ($x = 0.05$) shows better photocatalytic activity compared to pure TiO_2 and the other metal molybdate incorporated titanium dioxide $Cu_xMo_xTi_{1-x}O_6$ (CMT), $Zn_xMo_xTi_{1-x}O_6$ (ZMT) (for all cases, $x = 0.05$) for photodegradation of methyl orange (MO) under UV light irradiation. The methyl orange degradation is taken because it is chemically degraded faster than other dyes like rhodamine B (RB), thymol blue (TB), bromocresol green (BG), etc. The nano-sized photocatalyst were characterized by XRD, UV–vis spectra, BET surface area, UV–vis diffuse reflectance spectrum, EPR spectrum and TEM analyses.

2. Experimental

2.1. Preparation for nano-sized photocatalysts

2.1.1. Chemicals required

Titanium dioxide, $Ni(NO_3)_2{\cdot}6H_2O$, $(NH_4)_2MoO_4$, $Cu(NO_3)_2{\cdot}6H_2O$, $Zn(NO_3)_2{\cdot}6H_2O$, HNO_3 (65%), NH_4OH (25%), HF (40%), tartaric acid, triethanolammine (TEA), methyl orange (MO), rhodamine B (RB), thymol blue (TB), bromocresol green (BG) were A.R. reagents procured from B.D.H. of India.

2.1.2. Synthesis

The total synthesis was carried out in two steps by chemical solution decomposition method (CSD) reported by Pramanik and co-workers [22–24]. In the first step, the stock solutions of $Ni(NO_3)_2{\cdot}9H_2O$, $Cu(NO_3)_2{\cdot}6H_2O$, $Zn(NO_3)_2{\cdot}6H_2O$, $(NH_4)_2MoO_4$ and titanium tartarate solutions were prepared. In the second step, the equivalent amount of metal nitrate, $(NH_4)_2MoO_4$ and titanium tartarate solution were taken in a beaker as per chemical composition. The complexing agent TEA (triethanolamine) (where molecular ratio of metal ion:TEA = 1:3) was added to the homogeneous solution of constituents maintaining pH at 6–7 by nitric acid and ammonia. This mixed solution after evaporation and decompositions at 473 K, resulted in black carbonaceous light porous mass, which was followed by calcination in air at temperatures 823, 873 and 973 K for 2 h at a heating rate of 5 °/min for different chemical compositions. Complete synthesis procedure is presented below in Flowchart 1.

2.2. Photocatalytic experiment

Photocatalytic experiments were conducted using nano photocatalysts in presence of photocatalytically degradable different dyes in water solution. The photocatalytic reaction was carried out under irradiation of UV light ($\lambda > 280$ nm) from 400 W Ultrahigh-pressure Hg lamp (PHILIPS-HPL-N, G/74/2, MBF-400) with slow stirring of the mixture of solution of dye and ($M_xMo_xTi_{1-x}O_6$) (M = Ni, Cu, Zn; $x = 0.05$) photocatalysts by

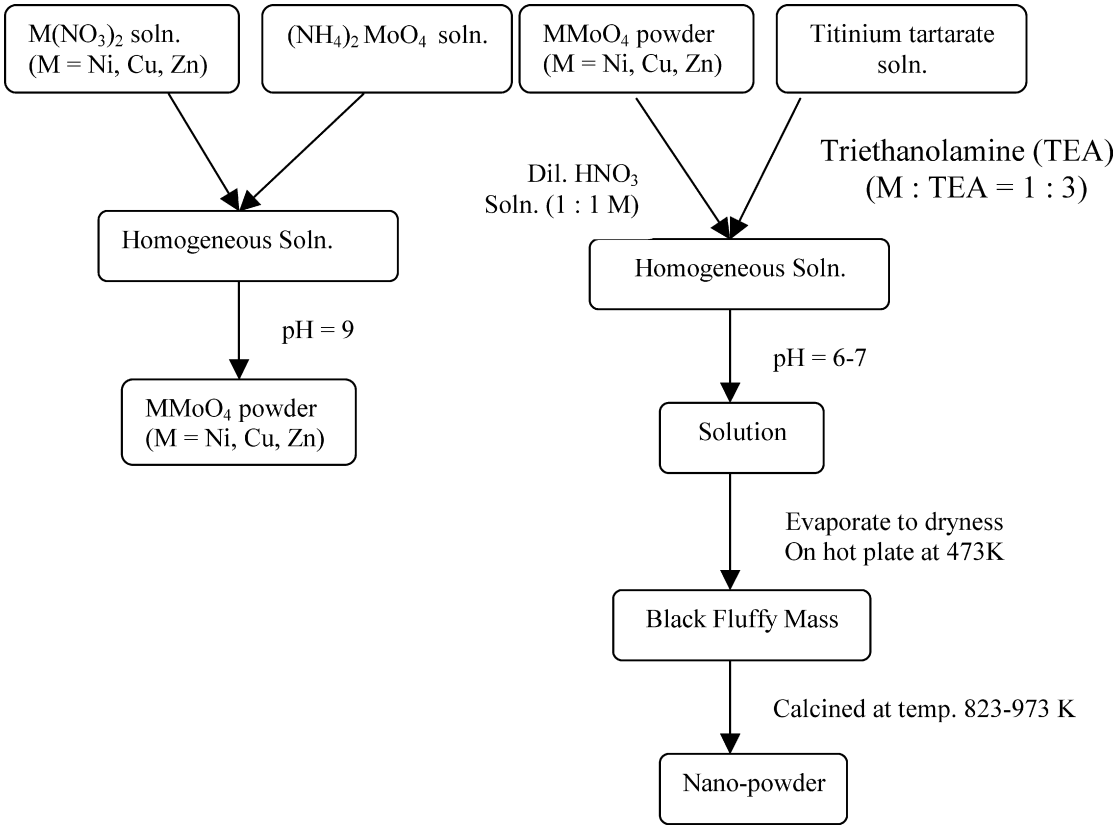

Flowchart 1. Synthesis of different metal molybdenum doped titanium dioxide ($M_xMo_xTi_{1-x}O_6$) (M = Ni, Cu, Zn; $x = 0.05$, 0.1, 0.5) nano photocatalysts.

magnetic stirrer, kept beneath the container of solution. The container was Petridis of volume 200 ml. The reactions were performed by adding nano powder of each photo catalyst (0.1 g) into each set of a 100 ml of different solution of dyes.

2.3. Analytical methods

A small volume (1 ml) of reactant liquid was siphoned out at regular interval of time for analysis. It was then centrifuged at 1100 rpm for 15 min, filtered through a 0.2 μm-millipore filter to remove the suspended catalyst particles and concentration of dye was measured by absorption spectrometry using UV–vis spectrometer (UV-1601, SHIMADZU) at its wavelength of maximum absorption.

3. Results and discussion

3.1. Characterization of the prepared powders

Characteristic XRD pattern from nickel molybdenum doped titanium dioxide $Ni_xMo_xTi_{1-x}O_6$ [when $x = 0.05$ (NMT1), 0.1 (NMT2) and 0.5 (NMT3)], $Cu_xMo_xTi_{1-x}O_6$ (CMT), $Zn_xMo_xTi_{1-x}O_6$ (ZMT), nickel doped TiO_2 [Ni–TiO_2 (NT)] and $NiMoO_4$ (NM) were observed in Fig. 1 at 550 °C. Six distinctive peaks of TiO_2 were found at 25.26°, 38.16°, 48.17°, 54.03°, 55.12° and 64.69° corresponding to reflection planes of crystal of the anatase (1 0 1), (0 0 4), (2 0 0), (1 0 5), (2 1 1) and (2 0 4), respectively (as per JCPDS 84 1285). No additional peaks were present, which could be assigned to the $NiMoO_4$ monoclinic phase, indicated that the resulting nano powder was alloy of nickel molybdate with titanium dioxide and all other metal molybdate doped TiO_2 were obtained in a pure anatase phase as revealed by XRD. Among all the metal, molybdenum doped titanium dioxide, only nickel molybdenum doped TiO_2 is reasonably photoactive (shown in Fig. 5(B)) compare the CMT and ZMT photocatalyst, against

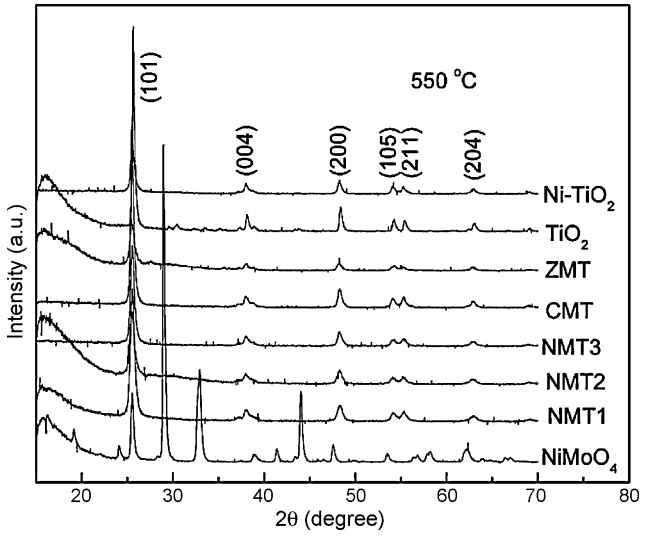

Fig. 1. XRD patterns of $NiMoO_4$ (NM), nickel molybdenum doped titanium dioxide (NMT1, NMT2, NMT3), CMT, ZMT, TiO_2 and Ni-TiO_2 (NT) photocatalyst at 550 °C.

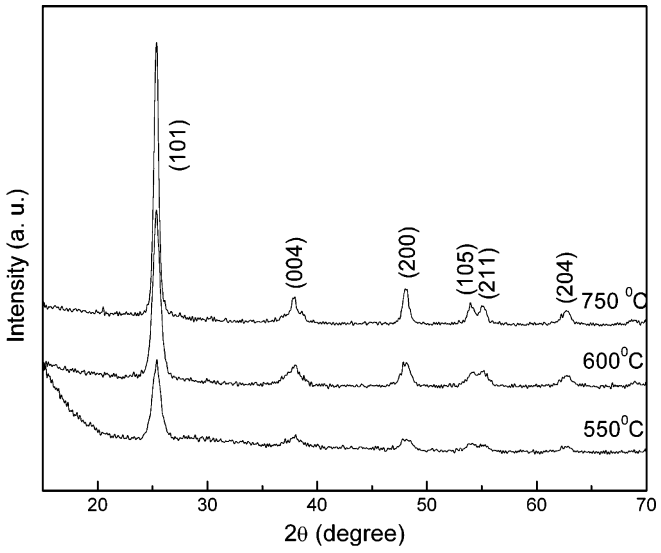

Fig. 2. XRD of $Ni_xMo_xTi_{1-x}O_6$ ($x = 0.05$) at different temperatures.

MO solution, for which we have concentrated our discussion mainly on $Ni_xMo_xTi_{1-x}O_6$ ($x = 0.05, 0.1, 0.5$) catalyst. The XRD patterns of $Ni_xMo_xTi_{1-x}O_6$ ($x = 0.05$) produced at different temperatures, indicated no change of crystallographic characteristics before and after the photocatalytic reactions shown in Figs. 2 and 3, respectively. Heating the samples above 973 K introduced the phase segregation of TiO_2 as pure anatase and $NiMoO_4$ as a monoclinic phase as noted by XRD.

3.2. Transmission electron microscopy (TEM) study

Nanoparticles with average size about 15 nm were observed in the transmission electron microscopy (TEM) (Model Philips TM-30, Philips Research Laboratories) of NMT1. This has been shown in Fig. 4, which is in good agreement with the average particle size of NMT about 11–13 nm obtained from XRD anal-

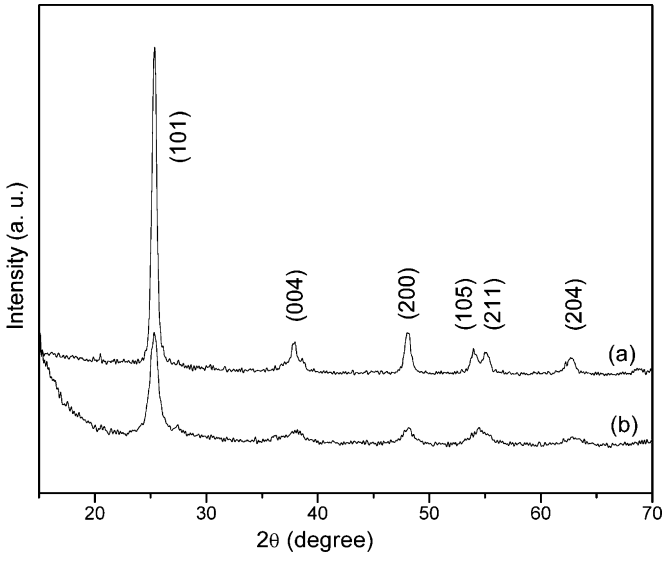

Fig. 3. XRD of $Ni_xMo_xTi_{1-x}O_6$ ($x = 0.05$) at 550 °C: (a) before and (b) after photocatalytic reaction with methyl orange solution.

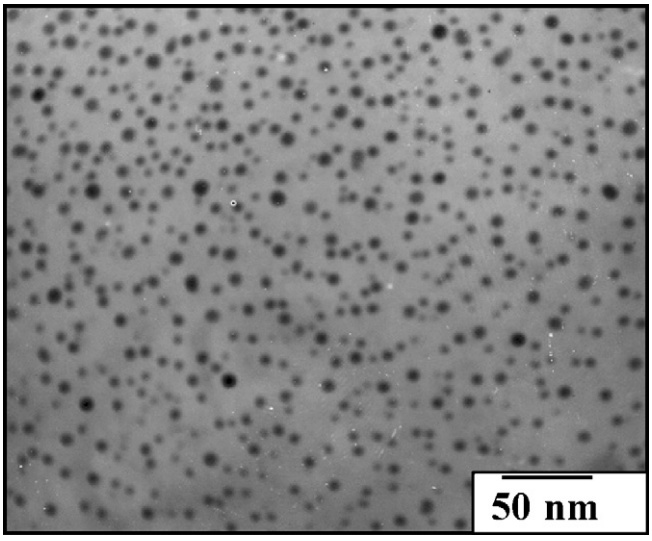

Fig. 4. Transmission electron microcopy of NMT1.

ysis (shown in Table 1). The TEM image of $Ni_xMo_xTi_{1-x}O_6$ ($x = 0.05$) indicated that the particles had narrow size distribution as analysed by software Image Tool. The catalyst had high specific surface area due to small particle sizes. This was also confirmed by BET surface area measurement by nitrogen adsorption and desorption. The large surface area enhanced photocatalytic activity through efficient adsorption of the reactant on the catalyst surface.

3.3. Specific surface area (BET) analysis

The specific surface areas (SSA) of different compositions of NMT1, NMT2, NMT3, P25 TiO_2, CMT, ZMT, NM and NT calcined at 550 °C temperatures are presented in Table 1, which were measured by dinitrogen adsorption-desorption isotherm in BECKMAN COULTER SA3100. It is noted that SSA decreases as dopant concentration of metal ions increases of a particular composition. The sample NMT1 having high specific surface area, which was about $145 \pm 5\ m^2/g$, provided good photocatalytic properties among all the photocatalysts against MO solution.

3.4. Photocatalytic activity of the prepared samples

Fig. 5(A) shows the maximum absorption wavelength of methyl orange at 464 nm under UV spectrometer and Fig. 5(B) shows effect of the dopant concentration on the photocatalytic activity of different metal molybdate doped titanium dioxide photocatalyst. From Fig. 5(B), it could be noted that the dopant concentration in TiO_2 has a great impact upon its photocatalytic activity to decolorize methyl orange solution. Table 2, shows the mode of color changes of different dyes in different

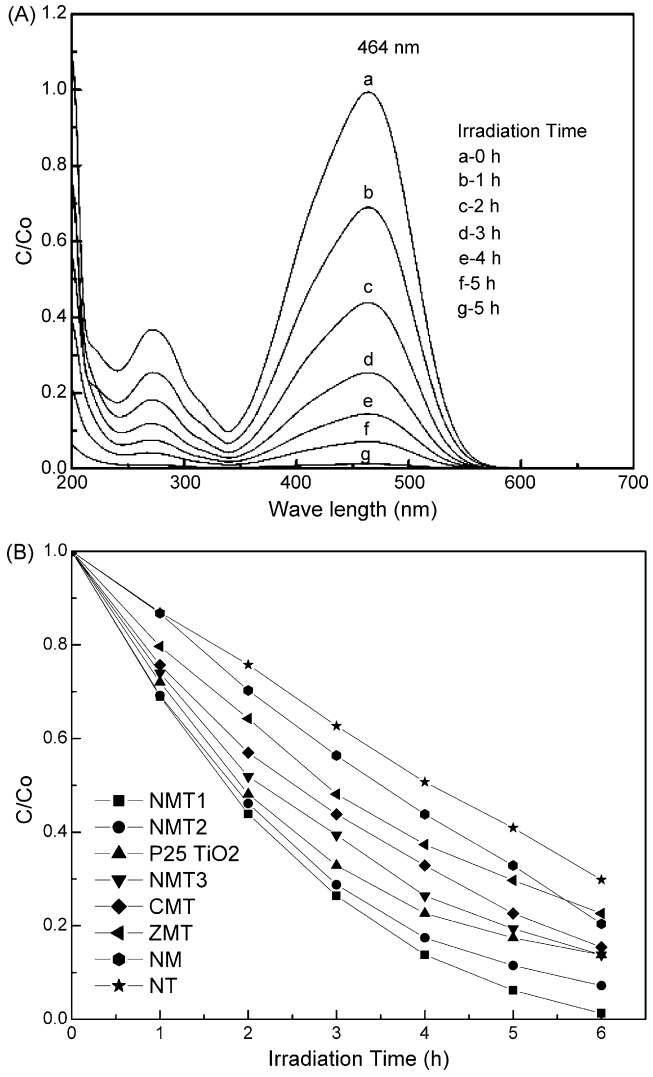

Fig. 5. (A) The changes in concentrations of methyl orange solution at 464 nm by the prepared sample calcined at 550 °C as a function of UV irradiation time. (B) The dopant concentrations of the catalyst are NMT1, NMT2, P25 TiO_2, NMT3, CMT, ZMT, $NiMoO_4$ (NM) and Ni-TiO_2 (NT).

Table 1
Resultant properties of NMT1, NMT2, NMT3, P25 TiO_2, CMT, ZMT, NM and NT composites

Sample	Reaction rate constant k (h^{-1})	S_{BET} (m^2/g)	Anatase crystal size (nm)	Bandgap energy (eV)
NMT1	4.44	149	11.85	2.66
NMT2	4.15	126	12.67	3.00
NMT3	3.10	126	11.95	3.06
P25 TiO_2	3.70	132	12.42	3.29
CMT	2.75	101	11.89	3.03
ZMT	2.18	68	17.08	3.01
NM	1.91	72	23.21	2.81
NT	1.40	48	24.49	3.10

Reaction rate constant, BET surface area measured by dinitrogen adsorption desorption isotherm at 550 °C.

Table 2
Time required for complete degradation of different dyes in different mole concentration in different pH

Different oraganic dyes	Initial color	Intermediate color	Final color	Concentration of the dyes ($\times 10^{-4}$ mol)	pH	Time required for complete degradation (h)
MO	Reddish-orange	Orange	Colorless	1.001	4.5	6
RB	Reddish-violet	Violet	Colorless	1.04	7.1	30
TB	Blue	Green	Colorless	1.07	9.5	13
BG	Blue	No change	No change	1.002	9.8	–

Time required for complete degradation of different dyes under the presence of ($Ni_xMo_xTi_{1-x}O_6$) ($x = 0.05$) and UV-light. MO, Methyl orange; RB, rhodamine B, TB, thymol blue, BG, bromocresol green.

mole concentration at different pH and time required for complete degradation of different dyes in the presence of NMT1 under Hg lamp. Among all of the dyes of MO, RB, TB and BG, methyl orange decolorization was fastest. The degradation rate constant (k) of MO using all the photocatalyst (time required for 50% decolorization of MO solution) are represented in Table 1. NMT1 showed the highest activity compared to the other photocatalysts. With the increase of the dopant concentration, the rate of photochemical reaction decreased and became ineffective after $x = 0.5$ for $Ni_xMo_xTi_{1-x}O_6$ alloy. Metal oxide incorporation influenced the photo reactivity of catalysts by acting as hole traps and probably by altering the e^-/h^+ pair recombination [25,26].

3.5. EPR spectrum study

From electronic paramagnetic resonance spectrum (EPR) of NMT shown in Fig. 6 under visible light irradiation on at 77 K in the presence of oxygen produced a signal at a g-tensor value of 2.001, indicating the presence of Ni^{+3} on irradiated TiO_2 [27].

This peak was absent in dark and no EPR signal was detected on pure TiO_2. This infers an effective transfer of photo-generated hole is trapped in Ni^{2+} producing Ni^{3+}, which facilitated the photochemical reaction subsequently.

3.6. UV–vis diffuse reflectance spectrum

The UV–vis diffuse reflectance spectrum of $NiMoO_4$ incorporated TiO_2 and pure TiO_2 presented in Fig. 7, gave distinct band-gap absorption edges at 465, 313, 305 and 387 nm for doped NMT1, NMT2, NMT3 and pure TiO_2 and corresponding band-gap energies are 2.66, 3.00, 3.06 and 3.20 eV, respectively. The UV–vis diffuse reflectance spectrum and band-gap energy of other compositions are shown in Fig. 7 and Table 1, respectively. With increasing the dopant concentration, the band gap increased, as a consequence the photocatalytic activities decreased. So, $Ni_xMo_xTi_{1-x}O_6$ ($x = 0.05$) photocatalysts has lower band-gap energy (2.66 eV) with highest photocatalytic activity compared to other dopant concentrations and P25 TiO_2.

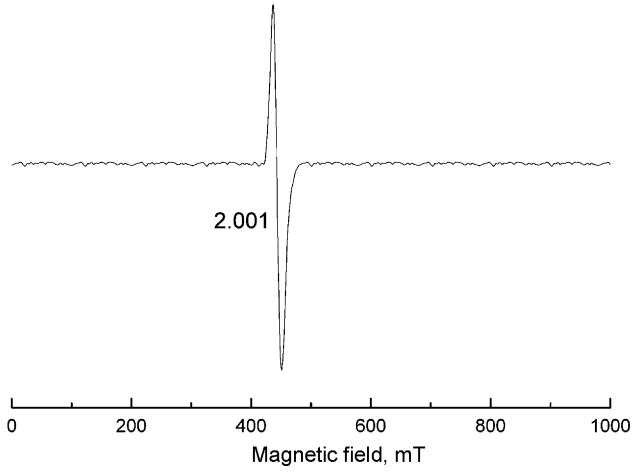

Fig. 6. EPR spectrum of NMT.

3.7. Mechanism

The detailed mechanism of the photo bleaching of dyes has been discussed in the literature [28–30]. It is well established that the conduction band electrons (e^-) and valence band holes (h^+) are generated when aqueous TiO_2 suspension is irradiated with light energy greater than its band-gap energy (E_g, 3.2 eV). When the methyl orange dye is irradiated with UV light, the dye is discolored within the time of reaction through the mutual contact between the dye and catalyst. The discoloration of the dye occurs because the dye is sensitized and the dye cation is formed. The dye cation is unstable and decomposes injecting an

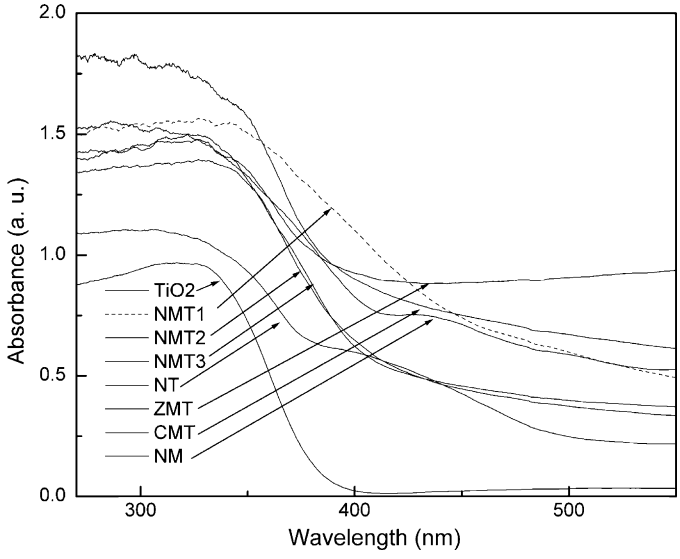

Fig. 7. UV–vis diffuse reflectance spectra of M-Ti samples with the highest dopant-atom content.

electron in the conduction band of TiO_2. This band-gap-electron starts the production of highly oxidative radical species through the formation of super oxide radical anion $O_2^{\bullet -}$ on the surface of the catalyst as long as the dye is present. In later steps of the reaction when long-lived colorless intermediates are present, the TiO_2 absorbs the light and produces the conduction-band-electron and valence-band-holes. Doped Ni^{2+} in these catalysts changes to Ni^{3+} with the localization of hole on the metal ion under irradiation of near UV light which efficiently reacts with intermediates of dye molecules.

4. Conclusion

In summary, photocatalyst $NiMoO_4$ (5 mol%) doped TiO_2 synthesized by CSD method is more photoactive than P25 TiO_2 and other metal molybdate doped TiO_2 due to high surface area, lower band-gap and photo chemical generation of Ni^{3+}. The dye is sensitized by the catalyst in presence of UV light and the dye cation is formed. The dye cation is unstable and decomposes injecting an electron on the conduction band of TiO_2. Electron goes to conduction band and hole is captured by Ni^{2+} producing Ni^{3+}, which has been noticed by EPR spectrum and helps to degrade the dye molecule faster.

Acknowledgement

The Council of Scientific and Industrial Research, India supported this work, for financial support.

References

[1] R. Villacres, S. Ikeda, T. Torimoto, B. Ohtani, J. Photochem. Photobiol. A: Chem. 160 (2003) 121–126.
[2] Y.-Q. Wang, L. Zhang, H.-M. Cheng, J.-M. Ma, Coll. Chem. Mol. Eng., Peking Univ. Beijing, Peop. Rep. China, vol. 21, no. 6, Gaodeng Xuexiao Huaxue Xuebao, 2000, pp. 958–960.
[3] H. Yamashita, M. Harada, J. Misaka, M. Takeuchi, K. Ikeue, M. Anpo, J. Photochem. Photobiol. A: Chem. 148 (2002) 257–261.
[4] G. Alhakimi, S. Gebril, L.H. Studnicki, J. Photochem. Photobiol. A: Chem. 157 (2003) 103–109.
[5] W.F. Yao, H. Wang, X.H. Xu, Y. Zhang, X.N. Yang, S.X. Shang, Y.H. Liu, J.T. Zhou, M. Wang, J. Mol. Catal. A: Chem. 202 (2003) 305–311.
[6] D. Dhak, S.K. Biswas, P. Pramanik, J. Eur. Ceram. Soc. 26 (2006) 3717–3723.
[7] S.D. Sartale, C.D. Lokhande, M. Muller, Mater. Chem. Phys. 80 (2003) 120–128.
[8] A. Tarafdar, P. Pramanik, Micropor. Mesopor. Mater. 91 (2006) 221.
[9] S. Roy, P. Pramanik, A. Singha, A. Roy, J. Appl. Phys. 97 (9) (2005), 094312/1-094312/6.
[10] H. Courbon, P. Pichat, J. Chem. Soc. Faraday Trans. 180 (1984) 3175.
[11] M.G. Kang, H. Hand, k. Kim, J. Photochem. Photobiol. 125A (1999) 119.
[12] W. Cun, Z. Jincai, W. Xinming, M. Bixian, S. Guoying, P. Ping, F. Jiamo, Appl. Catal. B: Environ. 39 (2002) 269–279.
[13] J.H. Carey, J. Lawrence, Bull. Environ. Contam. Toxicol. 16 (1976) 697.
[14] K. Yogo, M. Ishikawa, Catal. Surv. Jpn. 4 (2000) 83.
[15] J.C. Yu, L. Wu, J. Lin, P. Li, Q. Li, Chem. Commun. (2003) 1552–1553.
[16] S. Otsuka-Yao-Matsuo, M. Ueda, J. Photochem. Photobiol. A: Chem. 168 (2004) 1–6.
[17] Y. Inoue, Y. Asai, K. Sato, J. Chem. Soc. Faraday Trans. 90 (1994) 797–802.
[18] D. Beydoun, H. Tse, R. Amal, G. Low, S. McEvoy, J. Mol. Catal. A: Chem. 177 (2002) 265–273.
[19] Y. Inoue, T. Kubogawa, K. Sato, J. Phys. Chem. 95 (1991) 4059–4063.
[20] Z. Zhang, C. Wang, R. Zakria, J.Y. Ying, J. Phys. Chem. B 102 (1998) 10871–10878.
[21] W.F. Yao, H. Wang, X.H. Xu, X.F. Cheng, J. Huang, S.X. Shang, X.N. Yang, M. Wang, Appl. Catal. A: Gen. 243 (1) (2003) 185.
[22] A. Pathak, S. Mohapatra, S. Mohapatra, S.K. Biswas, D. Dhak, N.K. Pramanik, A. Tarafdar, P. Pramanik, Am. Ceram. Soc. Bull. 83 (8) (2004) 9301–9306.
[23] R.N. Das, P. Pramanik, Nanotechnology 15 (3) (2004) 279–282.
[24] T.K. Ghorai, D. Dhaka, A. Azizan, P. Pramanik, Mater. Sci. Eng. B 121 (2005) 216–223.
[25] J.G. Yu, X.J. Zhao, Q.N. Zhao, Thin Solid Films 379 (2000) 7–14.
[26] W. Choi, A. Termin, M.R. Hoffmann, J. Phys. Chem. 98 (1994) 13669.
[27] A. Gutierrez-Alejandre, J. Ramírez, G. Busca, Langmuir 14 (1998) 630–639.
[28] A. Houas, H. Lachheb, M. Ksibi, E. Elaloui, C. Guillard, J.M. Hermann, Appl. Catal. B: Environ. 31 (2001) 145.
[29] A. Bianco-Prevot, C. Baiocchi, M.C. Brussino, E. Pramauro, P. Savarino, V. Augugliaro, G. Marci, L. Palmisano, Environ. Sci. Technol. 35 (2001) 971.
[30] K. Tanaka, K. Padermpole, T. Hisanaga, Water Res. 34 (2000) 327.